In Situ Stress Determination, 3D Rock Properties and Numerical Modelling

Phil Dight[1]

[1] Professor of Geotechnical Engineering, Australian Centre for Geomechanics, The University of Western Australia, Crawley, WA, 6009,
phil.dight@uwa.edu.au

Abstract. In situ stress determination is possible using deformation rate analysis (DRA) without resorting to elastic theory and its constraints/assumptions. The approach is based on recovering the inelastic strain between two cycles of loading on cylindrical samples of rock. The test technique makes use of strain measurements in the axial and lateral direction conducted on subsamples recovered from oriented diamond drill core. The measurement of the normal stress on each of six uniquely oriented samples, provides a direct measurement of the in situ stress which can then be resolved in three dimensions using principal component theory (commonly called eigen analysis). The stress so determined can be evaluated at a 95% precision based on the number of samples tested (typically >18). A consequence of this approach is that the density, modulus, Poisson's ratio, P-wave and S-wave velocity and dynamic elastic properties can also be determined using the same principal component theory. This results in many of the rock properties being determined in three dimensions (3DRock) along with a 3D compliance matrix. Using the power of RS3®, numerical modelling of openings can be undertaken using the recovered in situ stress, the 3D rock properties and 3D compliance matrix. An example is provided of RS3® in identifying safety hazard awareness ahead of time.

Keywords: In situ stress, principal component theory, 3DRock, 3D compliance matrix

1 Introduction

Most often stress modelling focusses on the stress to strength relationship to identify areas of concern. Less often there is a focus on the deformation resulting from the excavation. When it comes to monitoring however it is deformation that is the only parameter that can be readily measured. Except for pillar deformation, the deformation measured in the field arises from the lateral strain/movement, not axial strain.

Stress modelling/analysis for operations without knowing the in situ stress, modulus and Poisson's ratio sounds like an oxymoron, yet the author has been presented with many such cases. Often the proponents will argue that they can readily undertake a sensitivity analysis, which further demonstrates their lack of understanding of the

R. Hammah et al. (eds.), *Proceedings of the Rocscience International Conference 2025 (RIC 2025)*, Atlantis Highlights in Engineering 40,
https://doi.org/10.2991/978-94-6463-900-1_7

environment in which they are working. In mining, the local tectonics dictate the in situ stress field. The in situ stress magnitude and orientation can change as well due to lithological influences such as density, modulus, and Poisson's ratio variations. One excuse proffered by practitioners has been that access to undertake the stress measurements underground is not available and/or stress measurements can be too expensive. To address the first point, in situ stress can be recovered from oriented drill core if the hole azimuth and plunge are known (such as exploration core), while the second point equates to the cost of about 5m of development. In this paper the in situ stress determination preferred for greenfield and brownfield sites by the author, comprises deformation rate analysis (DRA) [1-4]. A comprehensive guideline to the methodology and test procedure was published in 2016 [3] which has now been adopted in several laboratories (Russia, China, UK, and Australia). In our laboratory we have conducted tests on oriented core over depth ranges below surface from 200m to 3000m, for mining and civil projects from around the world.

A consequence of the approach taken for the in situ stress determination using DRA [5], has been the recovery of rock properties which have been shown to vary in three dimensions. In many cases around mineralized systems, this has opened up a Pandora's box challenging the orthodox approach to rock mechanics testing and analysis of rock core results which overwhelmingly assumes isotropic behavior and stress measurement governed by the elastic constitutive relationship. It is acknowledged that when anisotropy is visible testing considerations are adapted to measure the strength influence. But when it is not visible to the naked eye as in igneous and volcanic rocks it is most often ignored.

Further, from an appreciation of the 3D behavior of intact rock the development of the 3D compliance matrix can be derived. This can then be combined with an understanding of the 3D extension strain [5,6], allowing stress analysis of orthotropic intact rock and identification of strainburst [5]. Lastly, the lateral deformation can then be assessed and provides a basis for comparing deformation measured in the field, with the results from the numerical model.

2 Stress determination

Memory is a term usually attributed to live nature. Human memory is a cognitive process through which information is perceived, stored and retrieved, facilitating the encoding of past experiences and learning for future recall and utilization. Yet, certain materials possess the ability to retain "imprints" from prior treatments. This phenomenon provides the information which enables, under specific conditions, the reconstruction of the prior treatment and is regarded as "memory" [7, 8]. It has been demonstrated in the laboratory for instance, rocks can "remember" previously experienced stresses. This forms the basis for in situ stress measurements in the laboratory using rock cores extracted from underground space [9].

The most widely used methods for extracting rock memory are the acoustic emission (AE) method and DRA, which were proposed and started being used for in situ stress measurements in the early 1990s. When subjected to loading, solid materials produce internal microcracks, generating elastic waves from ultrasonic to sonic frequencies, a phenomenon known as “acoustic emission” [10]. Physical experiments demonstrate that under cyclic loading conditions, certain solid materials exhibit specific AE patterns: when the loading stress (2nd loading cycle in Fig. 1(a)) remains below the previously reached σ_0 (in the 1st loading cycle in Fig. 1(a)), the AE activity is negligible or close to background levels; conversely, it shows a significant increase (3rd loading cycle in Fig. 1(a) and (b)). This phenomenon was initially discovered by Kaiser in 1950 during tensile testing of metals and later termed the "Kaiser Effect" [11]. Since then the Kaiser Effect has been observed in cyclic compression tests of various rock materials, confirming that rocks retain the memory of stresses [10, 12, 13].

Different from the AE method, the DRA originated from the research field of Rock Mechanics, focusing on compression as the loading type. The DRA is based on measuring the difference in inelastic strain of rocks between two successive loading cycles (2nd and 3rd loading cycles in Fig. 1(c)) in uniaxial compression, as proposed by Yamamoto et al. [1]. Experimental evidence has shown that the stress at the inflection point in DRA plots (strain difference ($\Delta\varepsilon$) vs. axial stress (σ), Fig. 1(d)) corresponds to the maximum previous stress σ_0 (1st loading cycle in Fig. 1(c)). The mechanisms underlying the formation of inflection points can qualitatively be explained as follows: the inelastic rock strain produced by the first loading of DRA tests (2nd loading cycle in Fig. 1(c)) when exceeding the pre-stress is greater than that of the second loading (3rd loading cycle in Fig. 1(c)) due to the presence of residual strain. In other words, only when the loading is larger than the maximum previous stress can the internal pre-existing cracks in the rock have considerable frictional sliding or growth, resulting in inelastic deformation; this phenomenon is not evident or disappears when the maximum previous stress is exceeded again, which is similar to the Kaiser Effect. The main representation of this phenomenon is the appearance of inflection points in DRA plots (plots of strain difference vs. stress). Using either the AE method or DRA, the in situ stress along the orientation (known) of a single rock core can be reconstructed. The only difference is that using AE the expected stress in each sub direction must be known or assumed a priori whereas in DRA this is not the case, making the latter much more comprehensive and useful.

The need to determine stress concentration, types of instability and deformation response in excavations requires information about the 3D in situ stresses, modulus and Poisson’s Ratio. With DRA there is no assumption on the constitutive behavior of the rock and it is independent of elastic theory. Other stress measurement techniques (e.g. HI, hydraulic fracture) rely on isotropic elastic behavior to recover the stress. Isotropic behavior however, while it is a common assumption in rock mechanics, design is much less common. Further, when adopting hydraulic fracturing and borehole breakout to reconstruct the in situ stresses, a fundamental assumption is often made that one of the principal stresses is parallel to the borehole axis [14]. By contrast, the in situ stress measurements in the laboratory using rock memory effect, such as DRA, can measure the unknown 3D in situ stress tensor without presuming the direction and magnitudes of the principal stresses. Therefore, obtaining rock cores with a minimum of six different orientations (e.g. Fig. 2(c)) and conducting DRA tests, is necessary to determine the six independent components of the 3D stress tensor. Subsequently, the eigenvalues and eigenvectors of the 3D in situ stress tensor yield the magnitudes and directions of three principal in situ stresses (e.g. Fig. 2(d)), respectively [2]. However, drilling boreholes at various orientations at a great depth is usually challenging [15]. A common approach to resolve this difficulty is sub-coring, which involves drilling small rock cores along six different directions in full diameter diamond cores with known orientations recovered from the field [2,15,16], Fig. 2(a, b), and then preparation of the subcore specimens for DRA tests.

Table 1 summarizes some case studies of the in situ stress measurements using the DRA, with a focus on sizes and types of specimens. It is evident that in most studies, the oriented sub-cores were utilized to measure in situ stresses. Recently, a comparative analysis of deformation rate analysis using fullcore and subcore specimens has been conducted [17]. In general, the conclusion was that there was a size effect introduced as a result of expected surface disturbance on the larger samples, not present in the smaller samples. The difference in the stress determination was small, however, the larger samples were recovered from underground while the smaller samples are recovered by sampling the larger core. There is still further research needed in this area to ascertain the accuracy of the in situ stress measurement.

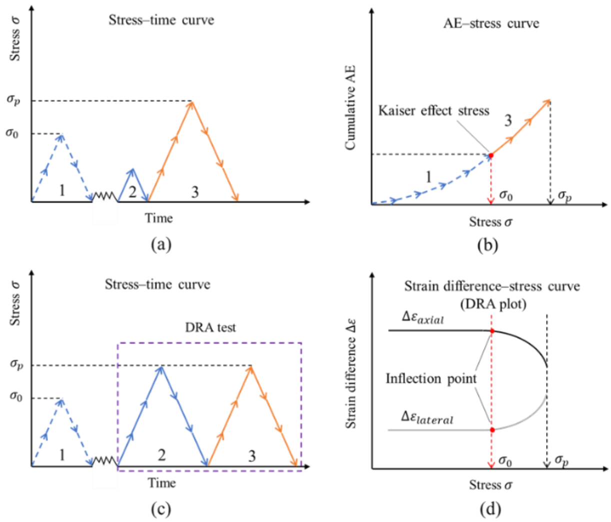

Fig. 1. Illustration of rock memory effect in AE method and DRA: (a) loading program (stress–time curves) of AE method (b) curves of cumulative AE events *vs.* stress (c) loading program (stress–time curves) of DRA (c) inflection points in DRA plots (strain difference–stress curves).

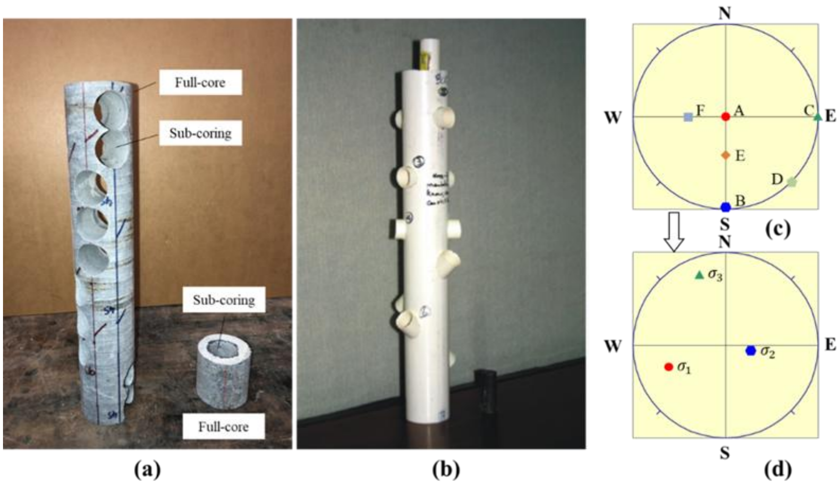

Fig. 2. Sub-coring full diameter diamond cores: (a) rock cores after sub-coring along different directions (b) model of sub-coring (c) example of sub-core orientation (after [2]) (d) example of the determined orientations of principal stresses.

Table 1. Summary of the in situ stress measurements using deformation rate analysis (DRA)

Year	Source	Type of project	Lithology	Specimen diameter (D) and height (H) (mm)	Type of Specimen	DRA loading regime	Reference
1990	Japan	-	Granodio-rite	D=18.5 - 18.8 H=40 - 45	Sub core	Uniaxial compres-sion	Yamamoto et al. [1]
1999	Japan Australia	Under-ground coal mine	Sandstone, coal, Granite, Sandy mudstone, Shale	-	Full-core	Uniaxial compres-sion	Seto et al. [18]
2002	Australia	Under-ground coal mine	-	D=20 H=45-50	Sub-core	Uniaxial compres-sion	Villaescusa et al. [16]
2006	Australia	Explo-ration core	Ultra-mafic, intrusive rock, quartzite	D=18-20 H=40-50	Sub-core	Uniaxial compres-sion	Dight et al. [2]
2010	Australia	Under-ground coal mine	-	D=18-20 H=40-50	Sub-core	Uniaxial compres-sion	Dight and Snyman [19]
2010	Portugal	Under-ground coal mine	Slate	D=50 H=125	Full-core	Uniaxial compres-sion	Xie et al. [20]
2013	Australia	Explo-ration core	Aplite porphyry, slate	D=18.5-18.8 H=40-45	Sub-core	Uniaxial compres-sion	Hsieh et al. [3]
2013	Taiwan	Water Tunnel	Chang-chikeng sandstone	D=22.8 H=46-48	Sub-core	Uniaxial compres-sion	Wu et al. [15]
2014	Iran	Hydro-electric power plant	-	D=23-24 H=46-48	Sub-core	Uniaxial compres-sion	Attar et al. [21]
2015	China	Oil field	Salt-gypsum rock	D=38 H=76	Sub-core	Uniaxial compres-sion	Ge et al. [22]
2021	Australia	Un-con-ven-tional gas	Shale	D=20.4-38.1	Sub-core	Uniaxial compres-sion	Fraser et al. [23]

		shale reservoir		H=39.5-76.4			
2022	Brazil	Open pit	Dolomite, Itabirite	-	Sub-core	Uniaxial compression	de Andrade Penido et al. [24]
2022	USA	Underground carbon sequestration	Shale, sandstone	D=30	Sub-core	Conventional triaxial compression	Higgins et.al. [25]
2023	USA	Geothermal project	Granitoid	D=30	Sub-core	Conventional triaxial compression	Bunger et.al. [26]

So in a project, if there is access to oriented core, then obtaining a measure of the in situ stress is possible and indeed advisable.

3 3D Rock properties

A benefit of the DRA approach to recovering the in situ stress using the approach by [5] is that the modulus and Poisson's ratio for each sub-sample can be measured. With six sub-core directions the principal components of modulus, Poisson's ratio, P-wave velocity, S-wave velocity, dynamic modulus and dynamic Poisson's ratio can be readily determined for the intact rock in three dimensions or combined to obtain average values. A consequence of this approach has been the identification of many igneous and volcanic rocks, which have no visible anisotropy being recognized as anisotropic [5]. In Table 2 there are seven sub-directions shown and 6 are subsequently used for the principal component analysis. The orientations are depicted in Fig. 3 as a stereographic projection. The results tabulated are an average of three tests each. A scan of the table shows some large variations in the mean results, in particular for modulus and Poisson's Ratio.

Table 2. Results of a comprehensive laboratory study

Sub sample	Trend	Plunge	σ1-σ3	E GPa	Poisson's ratio	E/M	V_p m/s	V_s m/s	E_{dyn} GPa	Poisson's ratio	σ_{ci} %	Tensile stress σ_i	K1c
A	202	28	234.5	93	0.23	0.81	6069	3696	91	0.16	42.7	42	1.8
B	22	62	115.9	80	0.25	0.87	5800	3595	86	0.16	64.7	17	1.5
C	292	0	227.8	54	0.14	0.65	5060	3291	67	0.09	23.6	19	2.3
D	317	39	277.6	52	0.12	1	5126	3325	70	0.11	14.1	18	1.9
E	202	73	260.8	94	0.18	0.77	6013	3465	82	0.20	40.3	27	1.6
F	153	19	296.4	80	0.19	0.86	5738	3435	78	0.15	11.8	34	2.0
G	87	39									55.0	21	1.9

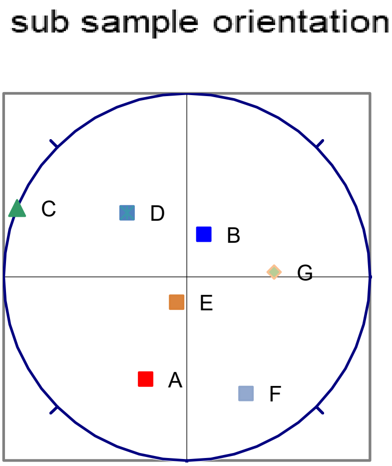

Fig. 3. Sub - sample directions

Table 3 disseminates the test results into the principal components. Shown also are the principal directions for each of the components, be they in situ stress, modulus, Poisson's Ratio, etc. Also shown are the ratios of maximum to minimum magnitudes. This is a Dacite and generally not considered to be anisotropic.

Table 3. Principal components of rock mechanics properties

Stress	Trend	Plunge	MPa
σ1	234	17	46
σ2	358	61	38
σ3	137	22	25
σ1:σ2:σ3	1.83 : 1.51 : 1.00		

Modulus	Trend	Plunge	GPa
E1	175	57	99
E2	31	27	83
E3	292	17	47
E1:E2:E3	2.10 : 1.76 : 1.00		

Poisson's Ratio	Trend	Plunge	
v1	40	33	0.27
v2	173	46	0.23
v3	292	25	0.10
v1:v2:v3	2.72 : 2.30 : 1.00		

Compliance data			
	GPa		
E_{11}	99	ν_{12}	0.25
E_{22}	83	ν_{13}	0.12
E_{33}	47	ν_{21}	0.29
G_{23}	27	ν_{23}	0.17
G_{13}	28	ν_{31}	0.06
G_{12}	36	ν_{32}	0.30
	Trend	Plunge	
	175	57	
	31	27	
	292	17	

Crack initiation	Trend	Plunge	%
σ_{ci1}	56	37	85.78
σ_{ci2}	185	40	38.49
σ_{ci3}	302	28	7.73
σ_{ci1}:σ_{ci2}:σ_{ci3}	11.09 : 4.98 : 1.00		

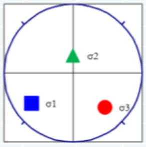

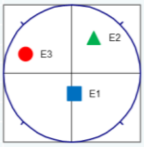

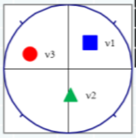

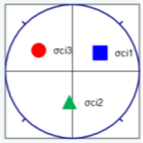

Stress

Poisson's ratio

Crack initiation stress

Legend – largest to smallest

Strength	Trend	Plunge	MPa
UCS1	334	24	285
UCS2	170	66	261
UCS3	67	6	171
UCS1:UCS2:UCS3	1.67 : 1.53 : 1.00		

E/M	Trend	Plunge	
E/M1	357	20	1.00
E/M2	208	67	0.80
E/M3	91	11	0.30
E/M1:E/M2:E/M3	3.33 : 2.67 : 1.00		

V_p	Trend	Plunge	m/s
Vp1	193	38	6077
Vp2	45	47	5974
Vp3	296	16	4924
Vp1:Vp2:Vp3	1.23 : 1.21 : 1.00		

BTS	Trend	Plunge	MPa
σt1	192	23	43
σt2	95	14	19
σt3	337	62	17
σt1:σt2:σt3	2.53 : 1.12 : 1.00		

Fracture toughness	Trend	Plunge	$MPa.m^{1/2}$
K1c1	290	8	2.26
K1c2	196	28	1.75
K1c3	34	61	1.45
K_{1c1}:K_{1c2}:K_{1c3}	1.56 : 1.20 : 1.00		

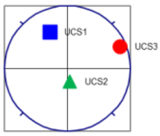

Strength

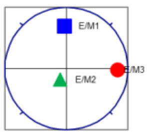

Loading modulus
Post peak modulus

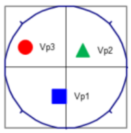

P-wave velocity

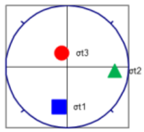

Brazilian tensile strength

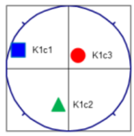

Fracture toughness results

4 Compliance Matrix

The mathematics of orthotropic materials has been well known [17] and is a feature of most finite element and finite difference programs. The input parameters of E, G, n and g however have not been easily obtained in 3D. In 2021 an approach was developed for recovering the orthotropic parameters from the testing of six uniquely oriented sub samples. The approach developed [Jeffcoat-Sacco, B. pers comm.] has been used in this study.

5 Extensional strain

A seminal paper on the relationship between the principal stresses and the development of extensional cracking (or tensile cracks for those that in the compression field)

[6] was published in 1981. The approach has been widely used to explain crack initiation and development leading to instability.

This was extended to 3 dimensions [5].

6 Summary

From oriented core (NQ diameter or greater), a minimum of six sub-samples with unique directions can be recovered from which to determine the in situ stress.

All tests (DRA, sc, st, K1c, E/M) are obtained from unconfined and triaxial testing of sub-core samples. This can be extended to cohesion and m_i in three dimensions if required.

Using Principal Component theory, the data can be resolved into the principal magnitudes and directions.

The data can then be used to determine the compliance matrix, and 3D extensional strain as presented in Table 4.

Table 4. The compliance matrix and 3D extensional strain

Compliance matrix

E_{xx}	99	GPa	v_{xy}	0.17	0.15
E_{yy}	81	GPa	v_{xz}	0.13	
E_{zz}	46	GPa	v_{yx}	0.20	0.18
G_{yz}	27	GPa	v_{yz}	0.16	
G_{xz}	26	GPa	v_{zx}	0.06	0.18
G_{xy}	33	GPa	v_{zy}	0.29	

	GPa		
E_{11}	99	v_{12}	0.17
E_{22}	81	v_{13}	0.06
E_{33}	46	v_{21}	0.17
G_{23}	27	v_{23}	0.16
G_{13}	26	v_{31}	0.06
G_{12}	33	v_{32}	0.29

Trend	Plunge
175	57
30	28
291	16

l	m	n
0.051	-0.5414	-0.8
0.435	0.7683	-0.5
-0.899	0.3414	-0.3

3D extensional strain

As we are looking at near surface exposures, $\sigma_3 = 0.0$ and we are considering the anisotropic behaviour, so

$\varepsilon_3=1/E_{33}*(-(\nu_{13}*\sigma_1)-(\nu_{23}*\sigma_2))$			
σ_1 (MPa)	50.0	ν_{13}=	0.06
σ_2 (MPa)	34.8	ν_{23}=	0.16
E_{33} (GPa)	45.5		
ε_3 =	-0.00027	Bursting >abs(0.0002)	

← **3D extensional strain**

7 Application

A mine requested a comprehensive study on the occurrence of strainburst in a dacite rock unit. The in situ stress was determined using DRA. The 3D properties were formulated using the above approach and an analysis performed using Rocscience RS3®, using the orthotropic option. A plot was generated of the expected 3D extensional strain based on a drive geometry provided by the mine.

In [6] it was considered that the critical strain would be 0.0002. A contour plot of the extensional strain is shown in Fig. 4. This indicates that the critical strain would occur in the floor of the drive with subsequent development in the wall adjacent. Note that this is all in the elastic range as appropriate for intact rock. The floor did indeed fail with rocks ejected subsequently from the sidewall as predicted before the event by this analysis. Fortunately, nobody was physically injured.

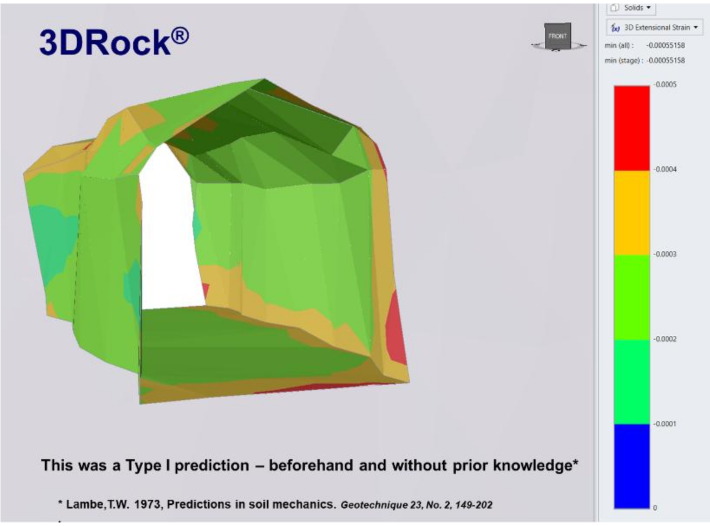

Fig. 4. Contours of extensional strain. The red areas would be expected to fail before the orange areas.

Now it is uncommon for support to be placed in the floor of a mine, which was the case in this operation.

This episode has proved pivotal in understanding where bursts can initiate. Subsequent studies have shown that the incidence of bursting increases when the rock is loaded to greater than 50% of the UCS or greater than σ_t/Poisson's ratio [27]. Each event causes a stress impulse which can lead to spalling/bursting.

8 Conclusions

The rock mechanics understanding of 3D behavior has been largely ignored by the geomechanics fraternity, where an almost total reliance on assuming isotropic behavior is a safe way to analyze. This study shows that it is possible and indeed desirable to harness the measurement of in situ stress, the development of 3D rock properties. The Rocscience program RS3® can provide a better picture of what would be expected to happen in development.

Acknowledgements
The project is a culmination of research work at the Australian Centre for Geomechanics. Contributors include Dr Ariel Hsieh, Dr Hongyu Wang, Dr Hijun Wang, Professor Arcady Dyskin, Professor Elena Pasternak and Broadus Jeffcoat-Sacco with the support of MRIWA and 13 major mining sponsors.

References

1. Yamamoto K, Kuwahara Y, Kato N, Hirasawa T (1990) Deformation rate analysis: A new method for in situ stress estimation from inelastic deformation of rock samples under uniaxial compressions. Tohoku Geophysical Journal 33: 127–47.
2. Dight PM (2006) Determination of in-situ stress from oriented core. ISRM Conference on In-Situ Stress. CRC Press, Boc Raton, pp 167–175
3. Hsieh A, Dyskin AV, Dight P (2013) The influence of sample bending on deformation rate analysis stress reconstruction. International Journal of Rock Mechanics and Mining Sciences 64:90–5.
4. Barr, SP (1993) The Kaiser effect of acoustic emissons for the determination of in-situ stress in the Carnmenellis Granite, PhD Thesis, University of Exeter.
5. Dight, PM (2023) Rock Properties to Predict Rockburst Vulnerability in Three Dimensions (Strainburst) MRIWA Project M0464, 2023.
6. Stacey, TR (1981) A simple extension strain criterion for fracture of brittle rock. International Journal of Rock Mechanics and Mining Sciences & Geomechanics Abstracts 18:469–474
7. Yamshchikov VS, Shkuratnik VL, Lavrov AV (1994) Memory effects in rocks. Journal of Mining Science 30:463–73.
8. Lavrov A (2005) Fracture-induced physical phenomena and memory effects in rocks: A review. Strain 41:135–49.
9. Hsieh A (2013). In situ stress reconstruction using rock memory. PhD Thesis. The University of Western Australia.
10. Goodman RE (1963) Subaudible noise during compression of rocks. Geological Society of America Bulletin 74:487–90.
11. Tensi HM (2004) The Kaiser-effect and its scientific background. Journal of Acoustic Emission 22:s1–s16.
12. Kurita K, Fujii N (1979) Stress memory of crystalline rocks in acoustic emission. Geophysical Research Letters 6:9-12.
13. Zhao K, Yang D, Huang Z, Gong C, Zeng P, Wang X, Li C, Zhao Y (2024) Investigations and new insights on the relation between the valid interval of the Kaiser effect and the characteristic stress. Earth-Science Reviews 249;104673.
14. Hudson JA, Harrison JP (2000) Engineering rock mechanics: an introduction to the principles: Elsevier Science, Kidlinton.
15. Wu J, Pan Y(2013) Three-dimensional in situ stress evaluation using a new under-coring technique: the Tseng-Wen Reservoir Transbasin water tunnel. Environmental earth sciences 68:77–86.
16. Villaescusa E, Seto M, Baird G (2002) Stress measurements from oriented core. International Journal of Rock Mechanics and Mining Sciences 39:603–15.
17. Amadei B (1983) Rock Anisotropy and the Theory of Stress Measurements. Lecture Notes in Engineering, (LNENG) vol 2. Springer-Verlag, Heidelberg. doi: 10.1007/978-3-642-82040-3
18. Seto M, Nag DK, Vutukuri VS (1999) In-situ rock stress measurement from rock cores using the acoustic emission method and deformation rate analysis. Geotechnical & Geological Engineering 17:241-66.
19. Dight P, Snyman L (2010) Stress measurement for St Barbara Mines Gwalia Deeps project–one of the world's deepest underground haulage mines. Mining Technology 119:246–54.
20. Xie Q, Qiu P, Yu X, Dinis da Gama C (2010) Initial-stress measurements with AE and DRA combined technique. Journal of China Coal Society 35:559–64.

21. Attar I, Ahmadi M, Nikkhah M, Attar A (2014) Investigating the capability of deformation rate analysis method in stress estimation: a case study of water conveyance tunnel of Gotvand Dam. Arabian Journal of Geosciences 7:1479–89.
22. Ge W, Zhang F, Chen M, Jin Y, Lu Y, Hou B (2015) Research on geotress measurement using DRA-Kaiser method in salt-gypsum formation. Yanshilixue Yu Gongcheng Xuebao34:3138-42.
23. Fraser D, Gholami R, Sarmadivaleh M (2021) Deformation Rate Analysis: How to determine in-situ stresses in unconventional gas reservoirs. International Journal of Rock Mechanics and Mining Sciences 146:104892.
24. de Andrade Penido H, Funato A, Metsugi H, Navarro Torres VF, Girao Sotomayor JM, Dight P, de Figueriredo RP, deAssis AP (2022) Application of the HF, DRA and DCDA technologies for in situ stress determination in Iron Quadrangle rock masses. Geomechanics and Geoengineering17:1670–94.
25. Higgins J, Lu Y, Benge M, Gunaydin D, Bunger A, Kelley M (2022) Triaxial Deformation Rate Analysis for Stress Estimation in the Sedimentary and Basement Rocks from the FutureGen Carbon Sequestration Project. In the 56th US Rock Mechanics/Geomechanics Symposium. ARMA, Westminster.
26. Bunger A, Higgins J, Huang Y, Hartz O, Kelley M (2024) Integration of triaxial ultrasonic velocity and deformation rate analysis for core-based estimation of stresses at the Utah FORGE geothermal site. Geothermics 120:103008.
27. Barton, N (2025) Reflections on an unrealistic continuum branch of rock mechanics – discontinuous behaviour alternatives. Rock Eng, 30p.